[7] "Electricity in patient care areas of hospitals," Nat. Fire Protection Ass., Quincy, MA, NFPA-76B, 1980.
[8] *8811A Bioelectric Amplifier Service Manual*, Med. Electron. Div., Hewlett-Packard Corp., Waltham, MA, 1971, p. 5.
[9] B. B. Winter and J. G. Webster, "Driven-right-leg circuit design," this issue, pp. 62–66.
[10] *78213 Neonatal Heart Rate Module Service Manual*, Med. Electron. Div., Hewlett-Packard Corp., Waltham, MA, 1977, p. 3.2.
[11] A. Miller, "Coupling circuit with driven guard," U.S. Patent 4 191 195, 1978.

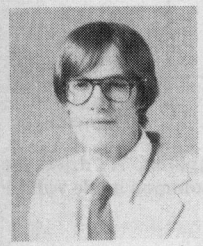

Bruce B. Winter (S'80) was born on July 8, 1958. He received the B.S. degree in electrical engineering from Montana State University, Bozeman, in 1980, and the M.S.E.E. degree from the University of Wisconsin, Madison, in 1981.

While at the University of Wisconsin, he was a Fellow and Teaching Assistant in instrumentation and logic design. Presently, he is working with large-scale integration at the IBM Corporation, Rochester, MN.

John G. Webster (M'59-SM'69) received the B.E.E. degree from Cornell University, Ithaca, NY, in 1953, and the M.S.E.E. and Ph.D. degrees from the University of Rochester, Rochester, NY, in 1965 and 1967, respectively.

He is a Professor of Electrical and Computer Engineering at the University of Wisconsin, Madison. In the field of medical instrumentation, he teaches undergraduate, graduate, and short courses, and does research on electrodes, impedance plethysmography, and portable arrhythmia monitors.

Dr. Webster is Associate Editor, Medical Instrumentation, of the IEEE TRANSACTIONS ON BIOMEDICAL ENGINEERING, and is a member of IEEE-EMBS Administrative Committee. He is coauthor, with B. Jacobson, of *Medicine and Clinical Engineering* (Englewood Cliffs, NJ: Prentice-Hall, 1977). He is Editor of *Medical Instrumentation: Application and Design* (Boston, MA: Houghton Mifflin, 1978). He is coeditor, with A. M. Cook, of *Clinical Engineering: Principles and Practices* (Englewood Cliffs, NJ: Prentice-Hall, 1979), with W. J. Tompkins, of *Design of Microcomputer-Based Medical Instrumentation* (Englewood Cliffs, NJ: Prentice-Hall, 1981) and, with A. M. Cook, of *Therapeutic Medical Devices: Application and Design* (Englewood Cliffs, NJ: Prentice-Hall, 1982).

Driven-Right-Leg Circuit Design

BRUCE B. WINTER, STUDENT MEMBER, IEEE, AND JOHN G. WEBSTER, SENIOR MEMBER, IEEE

Abstract—**The driven-right-leg circuit is often used with biopotential differential amplifiers to reduce common mode voltage. We analyze this circuit and show that high loop gains can cause instability. We present equations that can be used to design circuits that minimize common mode voltage without instability. We also show that it is important to consider the reduction of high-frequency interference from fluorescent lights when determining the bandwidth of the driven-right-leg circuit.**

INTRODUCTION

WHEN a differential amplifier records biopotentials, the voltage of the patient with respect to the amplifier's common is called the common mode voltage v_c. Since v_c can be transformed by the amplifier into an interfering differential signal [1], it is desirable to minimize v_c by attaching a third electrode to the patient. This electrode provides a low-impedance path between the patient and the amplifier common so that v_c is small. Connecting the electrode directly to the common is undesirable for two reasons. 1) If the circuit is not isolated, dangerous currents could flow through the third electrode. 2) A poor electrode contact may present up to 100 kΩ of resistance between the patient and the common.

The most common and effective use of the third electrode is to connect it to a driven-right-leg circuit [2], [3]. This circuit overcomes both of the problems listed above. It reduces the effective electrode resistance by several orders of magnitude, and it allows only a safe amount of current to flow through the third electrode. Although the circuit is used extensively in modern biopotential amplifiers [4]–[6], little has been written on optimal design technique. We present a design approach that results in the minimization of v_c. However, a nonoptimal driven-right-leg circuit may seem to work as well as one that minimizes v_c because: 1) the nonoptimal circuit reduces the interference to a level that is below the sensitivity of the recorder, or 2) other sources create more interference than v_c [7], [8].

Manuscript received January 18, 1982; revised July 23, 1982.

B. B. Winter was with the Department of Electrical and Computer Engineering, University of Wisconsin, Madison, WI 53706. He is now with the IBM Corporation, Rochester, MN 55901.

J. G. Webster is with the Department of Electrical and Computer Engineering, University of Wisconsin, Madison, WI 53706.

CIRCUIT DESCRIPTION

Fig. 1 shows the components of the driven-right-leg circuit. Resistors R_a and R_a average the voltage of the differential electrode pair to sense v_c. A_3 amplifies and inverts this voltage and feeds it back to the body via the third electrode. For ECG systems, the third electrode is commonly applied to the right leg; hence, we have the name driven-right-leg circuit.

Fig. 2 shows an equivalent circuit of the system shown in Fig. 1. The displacement current i_d that flows into the body via stray capacitances to nearby power lines divides between the current that flows directly to ground i_{d1} and the current that flows back to ground through the driven-right-leg circuit i_{d2}:

$$i_{d2} = i_d C_s/(C_s + C_b). \tag{1}$$

0018-9294/83/0100-0062$01.00 © 1983 IEEE

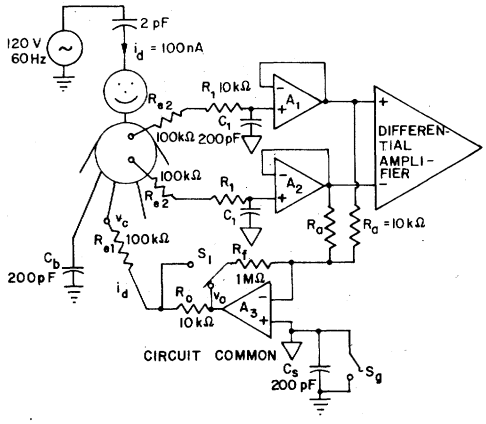

Fig. 1. A typical driven-right-leg circuit. A_3 drives v_c to a small value. With switch S_g open, the circuit represents an isolated amplifier with a stray capacitance to earth ground of C_s. C_b is the capacitance between the body and earth ground.

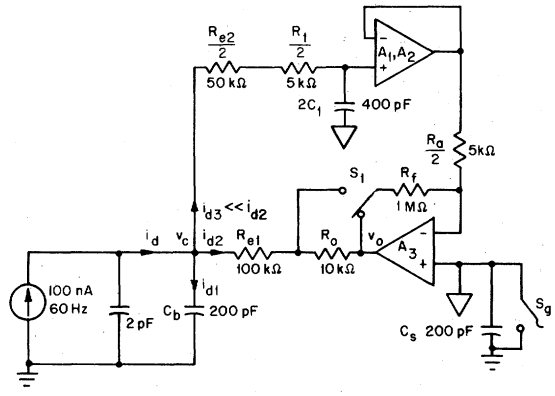

Fig. 2. Equivalent circuit of the system shown in Fig. 1. R_{e1} and R_{e2} represent the electrode resistances. Switch S_1 in the upper position represents a modified circuit which further reduces v_c by compensating for the voltage loss that occurs across R_0.

C_s is the stray capacitance between the amplifier common and earth ground and C_b is the stray capacitance between the body and earth ground. From Fig. 2,

$$v_0 = -Gv_c, \quad G = 2R_f/R_a \tag{2}$$

$$v_0 = v_c - (R_0 + R_{e1})\, i_{d2}. \tag{3}$$

G is the resistor ratio of the inverting amplifier, R_{e1} is the electrode resistance, and R_0 is a current-limiting resistor. From (2) and (3),

$$v_c = R_c i_{d2}, \quad R_c = (R_0 + R_{e1})/(G + 1). \tag{4}$$

If the third electrode is connected directly to common, the effective resistance between the patient and common is the electrode resistance R_{e1}. Equation (4) shows that if the third electrode is connected to a driven-right-leg circuit instead, and if $G > R_0/R_{e1}$, then this reduces the effective resistance to common R_c and thus reduces v_c.

Equations (1) and (4) show that v_c can also be reduced by decreasing the isolation capacitance C_s with respect to the body capacitance C_b. The main reason for providing good amplifier isolation, however, is for patient safety. NFPA standards require that less than 20 μA of current flow through the leads if line voltage appears on the patient [9]. If switch S_g of Fig. 1 is closed (i.e., there is no isolation from earth ground), then the designer must make sure that there is at least 6 MΩ (= 120 V/20 μA) of impedance between all of the amplifier leads and ground. R_0 may be increased to limit current flow through the driven-right-leg electrode, but under saturating voltage conditions, the input amplifiers A_1 and A_2 may break down and conduct dangerous currents. We found that with a typical electrode impedance of 10 kΩ, a typical op amp (MC1458) allowed 6 mA of current to flow under line voltage conditions. Most modern biopotential amplifiers meet the NFPA safety standards by having an isolation capacitance low enough to guarantee low current flow when line voltage appears anywhere on the isolated amplifier:

$$C_s < (20\ \mu\text{A})/(2\pi 60)\,(120\ \text{V}) = 440\ \text{pF}. \tag{5}$$

Thus, isolated amplifiers with $C_s < 440$ pF do not require R_0 to limit current flow from external sources. Many circuits that we have examined, however, include R_0 with ranges from 30 kΩ [4] to 1 MΩ [6]. Presumably, R_0 is included to protect the patient from transient currents that may flow from A_3 when the circuit is powered up. Weibell [10], however, has found that for duration of less than 200 ms, current flow of up to 5 mA (60 Hz) does not seem to pose a microshock threat.

If R_0 is included, then the driven-right-leg circuit is improved by switching switch S_1 of Figs. 1 and 2 to the upper position [11]. This circuit senses the output voltage at the electrode rather than at the op amp's output. Thus, the voltage at the electrode is $-Gv_c$, and the effective resistance to common R_c is independent of R_0:

$$R_c = R_{e1}/(G + 1), \quad G = 2R_f/R_a. \tag{6}$$

Equations (4) and (6) show that for $G \gg 1$, v_c is inversely proportional to G. Fig. 3 verifies this, and shows that the modified circuit of Figs. 1 and 2 (S_1 up) reduces v_c if R_0 is large. Fig. 3 also shows that to minimize v_c, we must maximize gain. We now examine circuit stability to determine the gain limit.

Circuit Stability

Fig. 4 shows the closed-loop components that may introduce the -180° of phase shift necessary for oscillation. A_1, A_2, and A_3 are compensated op amps. Since A_1 and A_2 have unity gain, they do not introduce substantial phase shift for the frequencies of interest. A_3, however, introduces a pole at $f = B/G$ Hz where B is the gain-bandwidth product of the op amp (typically 1-10 MHz) and G is the resistor ratio as defined by (6).

Fig. 4 also shows two RC stages that can each introduce -90° of phase shift in addition to the -90° introduced by the op amp. The series resistance of R_0 and R_{e1} forms a low-pass filter with the series combination of C_b and C_s. The circuit indicates a worst case phase shift because we have neglected the electrode capacitance which short circuits parts of the electrode resistance. R_1-C_1 is a low-pass filter that is usually included at the input of the input buffer. This filters out radio-frequency interference that could be demodulated by

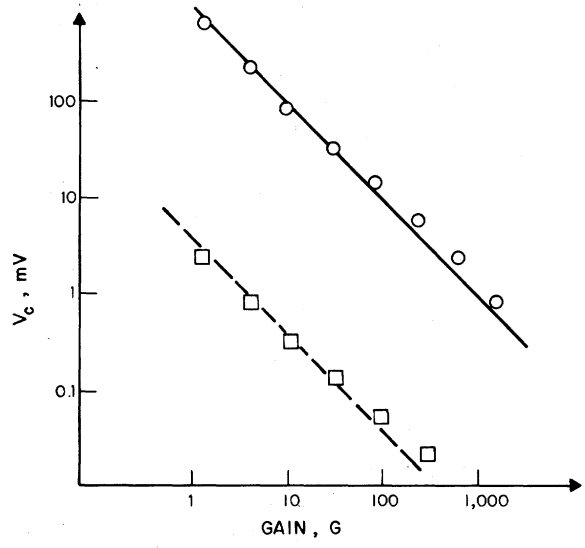

Fig. 3. v_c versus gain for the circuit of Fig. 2 with the conditions of i_{d2} = 100 nA, R_0 = 10 MΩ, and $R_{e1} = R_{e2}$ = 50 kΩ. For S_1 down, the solid line plots (3) and (4) and the circles show experimental data. For S_1 up, the dashed line plots (4) and (6) and the squares show experimental data.

the input buffers into interference at a frequency in the range of interest. This RC filter is not always included, however, because it decreases the effective CMRR of the amplifier at higher frequencies [1]. But even if R_1-C_1 were not purposely introduced, an RC stage exists at that point because the electrode resistance R_{e2} is shunted by capacitance between the electrode lead cable and common.

Ignoring the high-frequency pole of the unity gain amplifiers A_1 and A_2, the open-loop (S_2 open) transfer function for Fig. 4 is

$$\frac{v_{c2}}{v_{c1}} = \frac{G}{[1 + s/(2\pi f_a)]\,[1 + ks/(2\pi f_n)]\,[1 + s/(2\pi k f_n)]} \tag{7}$$

where

$$\begin{aligned} &G = 2R_f/R_a \\ &f_a = \text{corner frequency of driven-right-leg amplifier} = B/G \\ &B = \text{gain-bandwidth product of op amp } A_3 \\ &f_n = 1/[2\pi(\tau_1\tau_2)^{1/2}], \quad k = \zeta + (\zeta^2 - 1)^{1/2} \\ &\zeta = (\tau_1 + \tau_2 + \tau_3)\,\pi f_n, \quad \tau_3 = 2(R_0 + R_{e1})\,C_1 \\ &\tau_1 = (R_0 + R_{e1})\,(C_b C_s)/(C_b + C_s), \quad \tau_2 = (R_{e2} + R_1)\,C_1. \end{aligned} \tag{8}$$

τ_1 is the time constant for the first RC stage of Fig. 4, τ_2 for the second stage, and τ_3 relates how the second stage impedance loads the first stage. If we can ignore the loading effects that the second stage has on the first stage ($\tau_3 \ll \tau_1$ or $\tau_3 \ll \tau_2$), then (7) simplifies:

$$\frac{v_{c2}}{v_{c1}} = \frac{G}{[1 + s/(2\pi f_a)]\,(1 + s\tau_1)(1 + s\tau_2)}. \tag{9}$$

Circuit Design

To keep gain high and to avoid oscillation, we introduce compensation. We did not attempt lead compensation because, for it to be effective, we must have well-defined poles of the circuit. Because of variability in R_{e1}, R_{e2}, and C_b, we never know the exact location of the two RC poles, and thus we cannot guarantee pole cancellation.

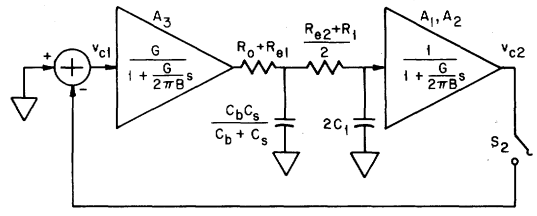

Fig. 4. This equivalent circuit of the driven-right-leg circuit shows the phase-inducing stages that may cause oscillation. B is the gain–bandwidth product of the op amps.

Thus, we use lag compensation. The simplest approach is to lower the corner frequency of the driven-right-leg amplifier f_a to f_{ac}. Since there is no reason to limit the dc gain, we replace the feedback resistor R_f with a capacitor C_f. As an example of how to calculate C_f, we assume the following values. These are higher than typical values to bring us closer to conditions that cause oscillation.

$$\begin{aligned} &C_s = 200\text{ pF}, \quad R_{e1} = R_{e2} = 100\text{ k}\Omega \\ &C_b = 200\text{ pF}, \quad R_0 = 10\text{ k}\Omega \\ &C_1 = 200\text{ pF}, \quad R_1 = 10\text{ k}\Omega. \end{aligned} \tag{10}$$

From (8),

$$\begin{aligned} &\tau_1 = 10\ \mu\text{s}, \quad \tau_2 = 20\ \mu\text{s}, \quad \tau_3 = 40\ \mu\text{s} \\ &k = 4.7, \quad f_n = 11\text{ kHz}. \end{aligned} \tag{11}$$

Since the two RC poles of (7) are more than a decade apart ($k^2 = 22$), then choosing f_{ac} such that the open-loop gain is less than or equal to unity at f_L as shown in Fig. 5 will guarantee at least a 45° phase margin:

$$f_{ac} \leqslant f_L/G_0 \tag{12}$$

where

$$\begin{aligned} &f_{ac} = \text{corner frequency of amplifier with } C_f \text{ feedback} \\ &\quad = 1/(\pi G_0 R_a C_f) \\ &f_L = \text{lowest } RC \text{ pole} \\ &\quad = f_n/k \\ &G_0 = \text{low-frequency open-loop gain of op amp } A_3. \end{aligned} \tag{13}$$

From (12) and (13),

$$R_a C_f \geqslant k/(\pi f_n) = 130\ \mu\text{s}. \tag{14}$$

If the two RC poles were less than a decade apart ($k^2 < 10$), then the open-loop gain at f_L would have to be less than one. Such would be the case if the isolation capacitance were large. Thus, we see that a low isolation capacitance may allow for high gain, and so the designer has one more good reason to increase amplifier isolation.

Bandwidth Considerations

We now consider the gain of the driven-right-leg circuit at frequencies other than 60 Hz [12]. R_1 and C_1 were added to attenuate frequencies above 100 kHz. Fluorescent light sources emit interference in the 1-10 kHz range. Fig. 6 shows

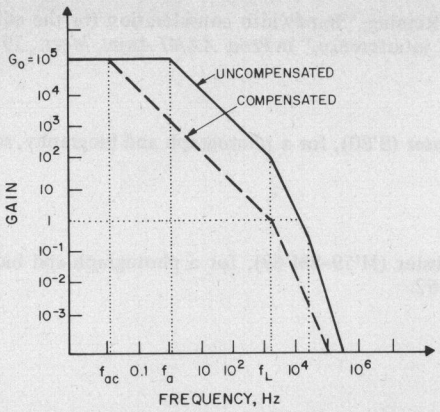

Fig. 5. Open-loop response described by (7) and (12). f_a has been lowered to f_{ac} so that the gain is unity at f_L. This guarantees at least a 45° phase margin.

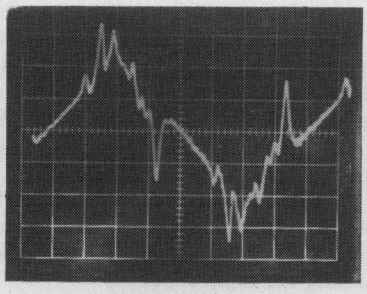

Fig. 6. Typical waveform interference from a fluorescent light source. The 1-kHz bursts occur at a 120-Hz rate. Time: 2 ms/div.

that the predominant interference is a 1-2 cycle burst of 1-kHz radiation that occurs at a 120-Hz rate. Typically, when a person is 1-2 m from a fluorescent light, this noise spike has an amplitude that is 10-50 percent as large as the 60-Hz interference. This 1-kHz content of v_c is transformed into interference more readily than the 60-Hz component because C_1 lowers the input impedance of the amplifier more for the higher frequencies, and thus degrades the amplifier's CMRR [1].

Many modern driven-right-leg circuits that we have examined do not satisfactorily reduce this 1-kHz content of v_c. Fig. 7 shows that a typical driven-right-leg circuit has a gain of 100 with a corner frequency of 100 Hz. Under most conditions, we have found that these circuits work well. But if the patient is within 1-2 m of a fluorescent source and the electrode impedances are large, then the 1-kHz bursts are often large enough to be transformed into 120-Hz interference by the nonlinearities of the recorder as shown in Fig. 8. When the bandwidth of the driven-right-leg circuit is increased, the interference is reduced as shown in Fig. 8.

The amount of 120-Hz interference that results from these 1-kHz bursts is also dependent on: 1) the degree of low-pass filtering that the signal undergoes, and 2) the bandwidth of the recorder. We made measurements on a typical isolated ECG amplifier with 200 pF of isolation capacitance and a single pole filter with a corner frequency at 200 Hz. We used a recorder with two poles at 80 Hz. For this system, a driven-right-leg circuit with a gain of 100 at 1 kHz will reduce interference from fluorescent lights to an acceptable level in all

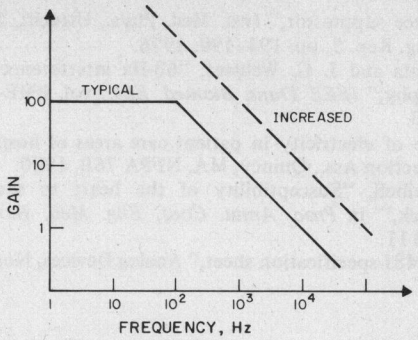

Fig. 7. Solid line: frequency response of typical driven-right-leg circuit. Dashed line: frequency response increased.

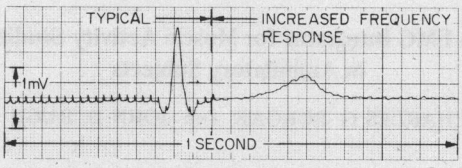

Fig. 8. Interference from a fluorescent light source on an ECG recording. Typical and increased frequency response shown.

but the very extreme cases (e.g., when the patient touches the light tube).

Conclusions

We examine circuit stability in order to determine the optimal design of the driven-right-leg circuit. While a nonoptimal circuit will work well for most recordings, high interference and/or sensitive recording requirements (such as the EEG) require an optimal circuit. An optimal circuit has the maximum gain permitted by the circuit stability equations. The designer must also tailor the frequency response of the circuit's gain to the reduction of interference from fluorescent lights.

Circuit stability is dependent on a number of variables such as isolation capacitance, the degree of RF filtering, and electrode resistances. Rather than present a set of circuit designs that cover all possible variable combinations, we have presented equations that define the circuit's poles. In this way, the designer can position the poles on a Bode plot to ensure stability.

References

[1] B. B. Winter and J. G. Webster, "Reduction of interference due to common mode voltage in biopotential amplifiers," this issue, pp. 58-62.

[2] "Patient safety," Med. Electron. Div., Hewlett-Packard Corp., Waltham, MA, Appl. Note AN718, 1971.

[3] M. R. Neuman, "Biopotential amplifiers," in *Medical Instrumentation: Application and Design*, J. G. Webster, Ed. Boston, MA: Houghton Mifflin, 1978.

[4] *78213A/C Neonatal Heart Rate Module Service Manual*, Hewlett-Packard Corp., Waltham, MA, 1977.

[5] *3000 Series Maintenance Manual*, Med. Syst. Div., General Electric Co., Milwaukee, WI, 1979.

[6] "MAC-1 microcomputer augmented cardiograph," Marquette Electronics, Milwaukee, WI, 1974.

[7] W. Sterken and G. J. van Keulen, "The evaluation of a mains-

interference suppressor," Inst. Med. Phys., Utrecht, The Netherlands, Prog. Rep. 5, pp. 194-199, 1976.
[8] J. C. Huhta and J. G. Webster, "60-Hz interference in electrocardiography," *IEEE Trans. Biomed. Eng.*, vol. BME-20, pp. 90-101, 1973.
[9] "Safe use of electricity in patient care areas of hospitals," Nat. Fire Protection Ass., Quincy, MA, NFPA 76B, 1980.
[10] F. J. Weibell, "Susceptibility of the heart to short-duration microshock," in *Proc. Annu. Conf. Eng. Med. Biol.*, vol. 20, 1978, p. 111.
[11] "Model 248J specification sheet," Analog Devices, Norwood, MA, 1980.
[12] W. N. Reining, "Bandwidth consideration for the elimination of '60 Hz' interference," in *Proc. AAMI Annu. Meet.*, 1977, p. 203.

Bruce B. Winter (S'80), for a photograph and biography, see this issue, p. 62.

John G. Webster (M'59-SM'69), for a photograph and biography, see this issue, p. 62.

Communications

An EMG Integrator for Muscle Activity Studies in Ambulatory Subjects

CHARLES G. BURGAR AND JOHN D. RUGH

Abstract—**A portable digital integrator is described for the measurement of electromyographic activity in the natural environment. Integrated muscle activity exceeding an adjustable threshold is accumulated and displayed on a seven digit LED readout in $\mu V \cdot s$. Technical specifications, schematic diagram, and application examples are provided.**

INTRODUCTION

Several musculoskeletal pain syndromes are believed to be a result of prolonged or excessive muscle activity [1]-[4]. Muscle hyperactivity is attributed to stressful life situations, habits, or one of several other factors such as bad posture, occupational demands, drug side effects, or cognitively mediated bracing. Experimental studies in the laboratory support the relationships between muscle hyperactivity and pain [5]-[8]; however, measurements in a patient's natural environment are necessary to verify these results.

Physiological data may be recorded in the patient's natural environment through several techniques. Telemetry systems have been described [9]-[11] which provide continuous analog data suitable for display on a chart recorder or storage on magnetic tape at the receiving station. Another technique involves the use of small FM tape recorders carried by the patient in his natural environment [12]-[15]. While these two recording techniques provide detailed data, they are not always convenient. The investigator is commonly faced with large amounts of data to analyze and the cost of most telemetry or FM recorder techniques often limits the investigator to studies of one or two subjects at a time. Finally, many musculoskeletal pain syndromes are cyclic in nature and therefore, may be several weeks or even months between exacerbations of the symptoms. It is difficult to justify devoting an elaborate recording system to one patient for such long periods.

Long-term investigations of muscle activity and myofascial pain carried out in our laboratory required an unobtrusive, portable, yet inexpensive EMG recorder which could be used by subjects in their natural environment over several weeks or months. Large numbers of subjects were to be recorded over extended periods and thus, simplicity of data reduction and analysis were essential. Preliminary studies indicated that cost effective data reduction could be achieved by integrating the raw EMG over specific time intervals before recording and by having patients record their own data. Rugh and Solberg [16] and Rugh [17], [18] described a portable EMG recording system employing an electrochemical integrator (E cell) for recording nocturnal muscle activity. While this instrument was found adequate for recording nocturnal EMG, the time required for the E-cell integrator to be "read out" made it impractical for daytime use where repeated readings were to be made. This paper describes a pocket-sized EMG integrator with a digital display for rapid readout.

Manuscript received September 10, 1981.

The authors are with the Health Sciences Center, University of Texas, San Antonio, TX 78284.

INSTRUMENT DESCRIPTION

The portable EMG integrator provides a seven-digit LED display of integrated muscle electrical activity. The instrument is calibrated to read in $\mu V \cdot s$ of muscle activity over time intervals ranging from a few seconds to 12 h. For simplicity of operation, only two front panel controls were made accessible to the subject: a power switch, which also serves to reset the digital integrator, and a push-button switch to read the display. A commercial portable timer [19] is used to signal the subject to record the reading at selected intervals. A threshold circuit is included which may be preset to eliminate postural muscle activity from the recordings when desired. The threshold is adjustable from 1 to 60 μV (average). The integrator accumulates total EMG activity whenever it exceeds the threshold and is linear (±5 percent) from 10 to 200 μV (180 Hz sinewave input).

Instrument-technical specifications and transfer functions were assessed using the test procedures described previously by us [20].

The input impedance is greater than 2 MΩ at 180 Hz. The frequency response is 100-310 Hz at the -3 dB points. Filter rolloff exceeds 12 dB per octave (36 dB per decade). Overall amplitude gain is 2000 (66 dB, ±1 dB). Input equivalent noise is less than 2 μV (rms). Sixty Hz suppression exceeds 90 dB. The common-mode rejection ratio at 60 Hz exceeds 80 dB, and at the geometric mean of the passband, exceeds 70 dB. Battery current consumption is less than 7 mA at 9 V. The overall physical dimensions are 3.0 X 5.9 X 1.1 in (7.5 X 15 X 2.8 cm), and the unit weighs 5.8 oz (164 g).

General Circuit Description

The block diagram shown in Fig. 1 gives a simplified view of instrument design. A differential amplifier is used to amplify

0018-9294/83/0100-0066$01.00 © 1983 IEEE